


RESEARCH

Open Access



# Diagnostic accuracy of coronary computed tomography angiography-derived fractional flow reserve

Wenbing Jiang<sup>1</sup>, Yibin Pan<sup>4</sup>, Yumeng Hu<sup>2</sup> , Xiaochang Leng<sup>2</sup>, Jun Jiang<sup>3</sup>, Li Feng<sup>2</sup>, Yongqing Xia<sup>2</sup>, Yong Sun<sup>3</sup>, Jian'an Wang<sup>3</sup>, Jianping Xiang<sup>2</sup> and Changling Li<sup>3\*</sup>

\*Correspondence:

lichl@edu.zju.cn

<sup>3</sup> Department of Cardiology,  
The Second Affiliated  
Hospital of Zhejiang  
University School  
of Medicine, 88 Jiefang Road,  
Hangzhou 310009, China  
Full list of author information  
is available at the end of the  
article

## Abstract

**Background:** Fractional flow reserve (FFR) is a widely used gold standard to evaluate ischemia-causing lesions. A new method of non-invasive approach, termed as AccuFFRct, for calculating FFR based on coronary computed tomography angiography (CCTA) and computational fluid dynamics (CFD) has been proposed. However, its diagnostic accuracy has not been validated.

**Objectives:** This study sought to present a novel approach for non-invasive computation of FFR and evaluate its diagnostic performance in patients with coronary stenosis.

**Methods:** A total of 54 consecutive patients with 78 vessels from a single center who underwent CCTA and invasive FFR measurement were retrospectively analyzed. The CT-derived FFR values were computed using a novel CFD-based model (AccuFFRct, ArteryFlow Technology Co., Ltd., Hangzhou, China). Diagnostic performance of AccuFFRct and CCTA in detecting hemodynamically significant coronary artery disease (CAD) was evaluated using the invasive FFR as a reference standard.

**Results:** Diagnostic accuracy, sensitivity, specificity, positive predictive value (PPV) and negative predictive value (NPV) for AccuFFRct in detecting  $FFR \leq 0.8$  on per-patient basis were 90.7, 89.5, 91.4, 85.0 and 94.1%, respectively, while those of CCTA were 38.9, 100.0, 5.71, 36.5 and 100.0%, respectively. The correlation between AccuFFRct and FFR was good ( $r = 0.76$  and  $r = 0.65$  on per-patient and per-vessel basis, respectively, both  $p < 0.0001$ ). Area under the curve (AUC) values of AccuFFRct for identifying ischemia per-patient and per-vessel basis were 0.945 and 0.925, respectively. There was much higher accuracy, specificity and AUC for AccuFFRct compared with CCTA.

**Conclusions:** AccuFFRct computed from CCTA images alone demonstrated high diagnostic performance for detecting lesion-specific ischemia, it showed superior diagnostic power than CCTA and eliminated the risk of invasive tests, which could be an accurate and time-efficient computational tool for diagnosing ischemia and assisting clinical decision-making.

**Keywords:** Coronary computed tomography angiography, Fractional flow reserve, Computational fluid dynamics, CT-derived FFR



## Introduction

Accurate diagnosis of stenosis severity is essential for doctors in therapeutic decision-making regarding the need for percutaneous coronary intervention (PCI) or coronary artery bypass grafting (CABG). Coronary computed tomography angiography (CCTA) has emerged as a useful tool for evaluating coronary artery disease (CAD) severity [1]. However, the anatomic information obtained by CCTA is unable to ultimately reflect the physiological and physical influence on blood flow, which results in the poor correlation between lesion-specific ischemia and stenoses detected by CCTA [2–4]. Invasive fractional flow reserve (FFR), which assesses the ratio of flow across stenoses to putative flow in the absence of stenosis, is a well-established reference standard for evaluating the ischemic potential of individual lesions [5, 6]. Several validation studies have demonstrated that FFR-guided coronary intervention can enhance survival and reduce unnecessary revascularization [3, 7]. Despite the clinical benefits of FFR, the cost and potential complication of a pressure wire limited the wide application of FFR. Thus a tool that could precisely calculate the FFR value inexpensively would benefit more people in the world.

Computational fluid dynamics (CFD), as applied to CCTA images, represents a novel technique for assessing the physiological significance of CAD [8]. CT-derived FFR can be computed non-invasively from standard CCTA images without modifying acquisition protocols or additional imaging, and it has been validated in several trials with good diagnostic performance [9–11]. CT-FFR involves coronary segmentation, estimation of blood flow, numerical solving for the flow field across a coronary tree, etc. The complexity of these steps results in the most significant restriction of CT-FFR, namely time-consuming. In the FFR<sub>CT</sub> computation process, parallel supercomputers are needed [12]. Thus, a CT-derived FFR approach without high computational demands becomes very attractive.

In this study, a novel CT-derived FFR method, AccuFFRct, which efficiently computes lesion-specific non-invasive FFR based on anatomic and functional information, was used to assess its feasibility and diagnostic accuracy with wire-based FFR as a reference standard.

## Results

### Patient characteristics

The study population consisted of 54 patients with 78 vessels, including 34 males and 21 females. 45 (58%) lesions were located in left main or left anterior descending arteries, 10 (13%) were in left circumflex arteries and 14 (18%) were in right coronary arteries, there were 9 multi-vessel lesions. Detailed patient baseline characteristics are summarized in Table 1.

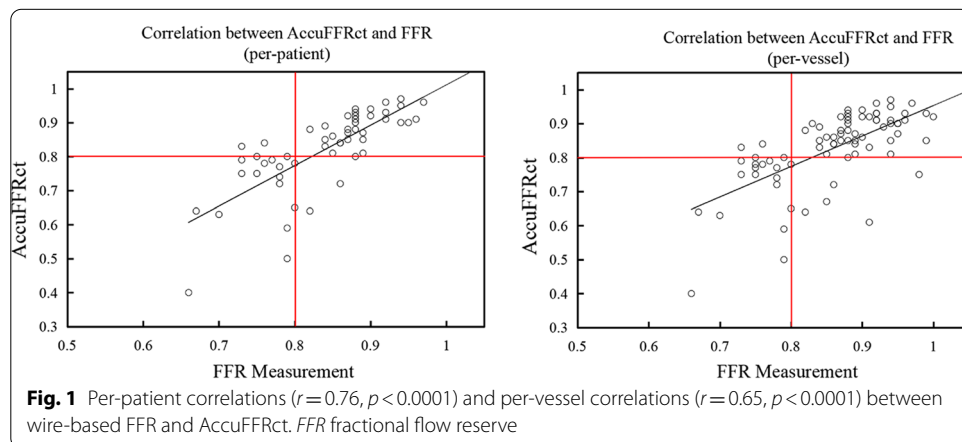
### Correlation and agreement between AccuFFRct and invasive FFR

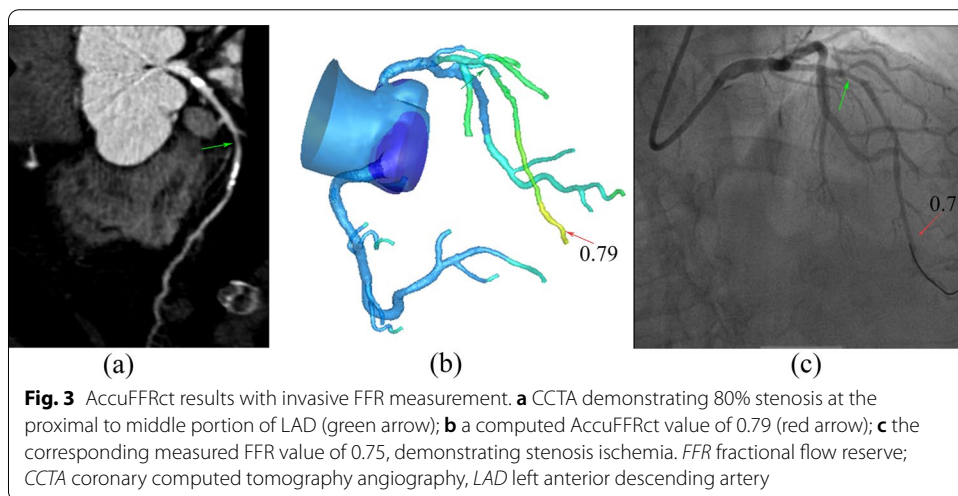
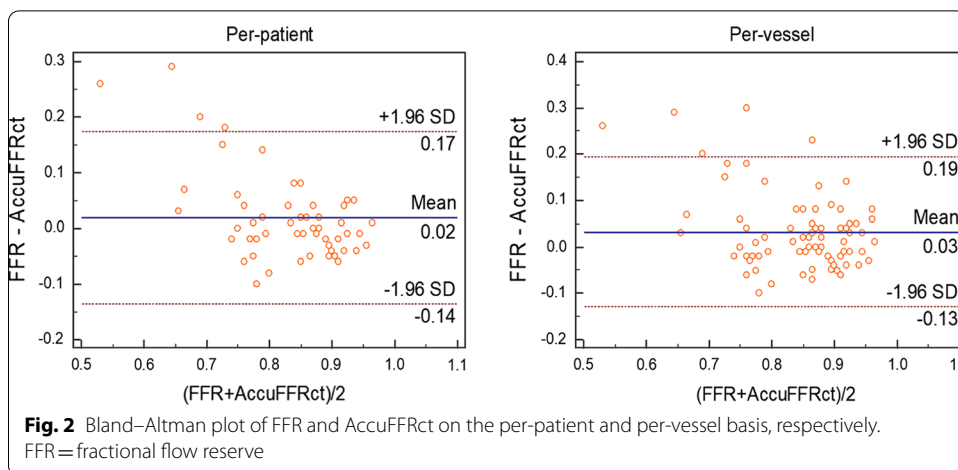
The correlation and agreement between AccuFFRct and FFR on a per-patient and per-vessel basis are shown in Figs. 1 and 2, respectively. Good correlation (Pearson's correlation coefficient  $r = 0.76$  and  $0.65$ ,  $p < 0.0001$ ) and agreement (mean difference

**Table 1** Patient baseline characteristics

| Parameter                            | Number of patients (54) |
|--------------------------------------|-------------------------|
| Age (y)                              | 65 ± 8                  |
| Male sex                             | 63% (34)                |
| Weight (kg)                          | 66 ± 11                 |
| Height (cm)                          | 165 ± 8                 |
| Body mass index (kg/m <sup>2</sup> ) | 24 ± 3                  |
| Cardiovascular risk factors          |                         |
| Systolic blood pressure (mm Hg)      | 131 ± 20                |
| Diastolic blood pressure (mm Hg)     | 76 ± 14                 |
| Angina pectoris                      | 20% (11)                |
| Diabetes                             | 19% (10)                |
| Hypertension                         | 57% (31)                |
| Hyperlipidemia                       | 7% (4)                  |
| Coronary CT angiography              |                         |
| Agatston score, % (n)                |                         |
| 0–399                                | 69% (37)                |
| 400–799                              | 22% (12)                |
| > 799                                | 9% (5)                  |
| CCTA stenosis ≥ 50% (patient)        | 56% (30)                |
| CCTA stenosis ≥ 50% (vessel)         | 65% (51)                |
| AccuFFR ≤ 0.80 (patient)             | 37% (20)                |
| AccuFFR ≤ 0.80 (vessel)              | 32% (25)                |
| Vessel location, % (n)               |                         |
| LM/LAD                               | 58% (45)                |
| LCX                                  | 13% (10)                |
| RCA                                  | 18% (14)                |
| Multi-vessels                        | 11% (9)                 |
| Stenosis degree, % (n)               |                         |
| < 50%                                | 43% (23)                |
| ≥ 50%                                | 57% (31)                |
| FFR ≤ 0.8                            | 41% (22)                |

CT computed tomography, CCTA coronary computed tomography angiography, LM left main artery, LAD left anterior descending artery, LCX left circumflex artery, RCA right coronary artery, FFR fractional flow reserve





0.06 ± 0.07) were observed. Representative patient case from the study is shown in Fig. 3.

The average AccuFFRct was 0.83 ± 0.10. Among all 78 vessels, there were 20 true positives (TP), 50 true negatives (TN), 6 false positives (FP), and 2 false negatives (FN) using FFR as the reference standard. With AccuFFRct ≤ 0.8 taken as the cut-off value of ischemia-causing stenoses (FFR ≤ 0.8), the sensitivity, specificity, positive predictive value (PPV) and negative predictive value (NPV) of AccuFFRct for diagnosis of ischemia-causing stenoses on the per-patient basis were 89.5, 91.4, 85.0, and 94.1%, respectively. The diagnostic accuracy was 90.7%. For the per-vessel assessment, the diagnostic accuracy, sensitivity, specificity, PPV, and NPV for AccuFFRct were 89.7, 90.5, 89.5, 76.0 and 96.2%, respectively. Detailed information of diagnostic performance of AccuFFRct is summarized in Table 2. When using CCTA only to predict FFR ≤ 0.8, the accuracy, sensitivity, specificity were 38.9, 100.0, 5.7% on per-patient basis and 32.0, 100, 7.0% on per-vessel basis, respectively. It is notable that AccuFFRct showed much better diagnostic performance in detecting ischemia-causing stenoses than the traditional assessment by CCTA. The extremely low specificity and accuracy of CCTA means overestimation of

**Table 2** Diagnostic performance of AccuFFRct for the prediction of ischemia of lesion on a per-patient and per-vessel level

| Parameter                      | AccuFFRct $\leq 0.80$ [95% CI] | AccuFFRct $\leq 0.80$ [95% CI] |
|--------------------------------|--------------------------------|--------------------------------|
| Per-patient level ( $n = 54$ ) | Per-vessel level ( $n = 78$ )  |                                |
| Accuracy                       | 90.7 [79.7–96.9]               | 89.7 [80.8–95.5]               |
| Sensitivity                    | 89.5 [66.9–98.7]               | 90.5 [69.6–98.8]               |
| Specificity                    | 91.4 [76.9–98.2]               | 89.5 [78.5–96.0]               |
| PPV                            | 85 [65.5–94.4]                 | 76 [59.5–87.2]                 |
| NPV                            | 94.1 [81.1–98.3]               | 96.2 [87.20–98.9]              |

Data are shown in percentage with raw data in parentheses and 95% confidence interval in brackets. *CI* confidence interval, *NPV* negative predictive value, *PPV* positive predictive value

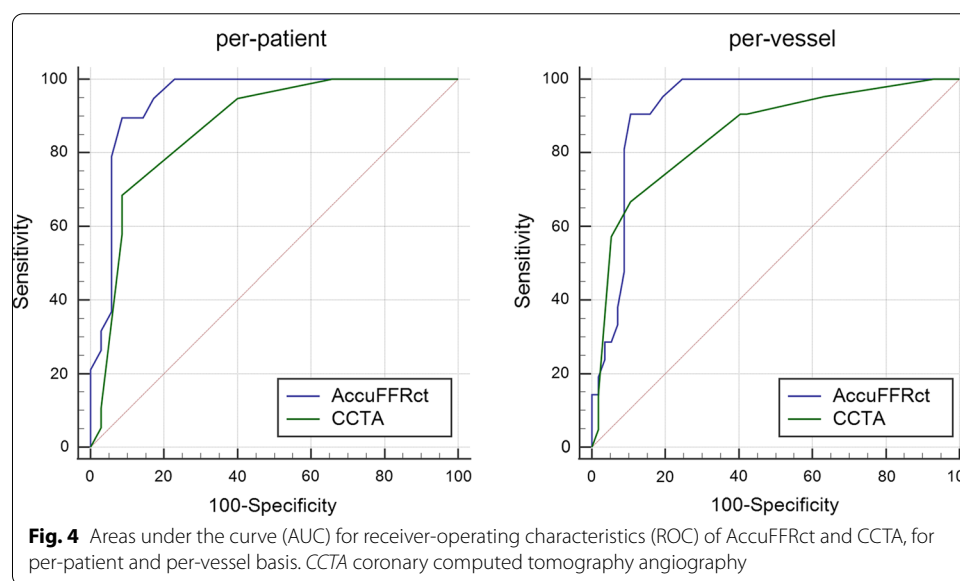


**Fig. 4** Areas under the curve (AUC) for receiver-operating characteristics (ROC) of AccuFFRct and CCTA, for per-patient and per-vessel basis. *CCTA* coronary computed tomography angiography

lesion severity, which may lead to unnecessary downstream invasive tests or intervention therapies. The high accuracy, sensitivity, specificity of AccuFFRct means it can get accurate assessment of coronary stenoses in most of cases without obvious underestimation or overestimation.

The ROC curves of AccuFFRct and CCTA on a per-patient and per-vessel basis are shown in Fig. 4. For a per-patient basis, the AUC for AccuFFRct and CCTA was 0.945 vs. 0.870, while for a per-vessel basis, the AUC for AccuFFRct and CCTA was 0.925 vs. 0.853. This also showed the superior diagnostic ability of AccuFFRct in identifying whether a stenosis can lead to ischemia.

### Discussion

We have developed a novel method that allows fast computation of FFR from CCTA images alone. In the study on a population of 54 patients with stenoses in 78 coronary vessels, AccuFFRct showed a good correlation with Pearson’s correlation coefficient  $r = 0.76$  ( $p < 0.001$ ) and agreement with invasive FFR. The overall diagnostic accuracy of AccuFFRct in predicting hemodynamically significant CAD (defined by  $FFR \leq 0.80$ ) was 90.7 and 89.7% on a per-patient and per-vessel basis, respectively. In this population, the

accuracy of CCTA was only 61.8 and 58.1% for per-patient and per-vessel, respectively. The diagnostic accuracy of AccuFFR<sub>ct</sub> is much higher than CCTA in the functional evaluation of lesion-specific ischemia. The cause is that CCTA often overestimates stenosis severity, and existing studies showed that less than 50% of CCTA-defined severe stenoses caused ischemia [2, 13]. Considering both anatomic and functional information, AccuFFR<sub>ct</sub> can comprehensively assess the influence of stenoses on blood flow and facilitate clinical decision-making.

CT-derived FFR methods can estimate FFR from typically acquired CCTA images without additional image acquisition, CCTA protocols, and medication administration modification. The diagnostic performance of such approaches has been validated and verified [9–11, 14, 15]. A 3D CT-FFR technique (FFR<sub>CT</sub>, Heartflow) exhibited good correlations with invasive FFR, with diagnostic accuracy ranging from 73 to 86% and AUCs of FFR<sub>CT</sub> in detecting lesion-specific ischemia ranging from 0.81 to 0.90 [9–11]. FFR<sub>CT</sub> showed excellent diagnostic performance compared with CCTA, SPECT and PET and reduced more than one-half ICA in clinical practice [16, 17]. Hlatky et al. [18] demonstrated that the use of FFR<sub>CT</sub> to guide ICA planning and revascularization could reduce costs and improve clinical outcomes. Furthermore, a recent trial including 5083 patients represented that FFR<sub>CT</sub> could provide much more useful information for clinical decision-making and FFR<sub>CT</sub>-guided patient management enhanced one-year survival free of major adverse cardiac events [19, 20]. Besides, Siemens Healthcare [15] reported a new approach for computing cFFR from CCTA images using a reduced-order CFD model. The correlation of cFFR and invasive FFR ranged from 59 to 75% and the AUCs varied from 0.83 to 0.92 [15, 21, 22]. The machine learning (ML)-based cFFR was the latest version of the CT-FFR approach developed by Siemens Healthcare [23]. This algorithm learned the output of the CFD model and CCTA anatomies. Validation studies [12, 24] showed that the highest diagnostic accuracy of ML-based cFFR was 85%, with the sensitivity, specificity, PPV and NPV of 89, 76, 89 and 77%, respectively. The highest AUC of ML-based cFFR was 0.84. A more recent CT-FFR study ( $\mu$ CT-FFR) using transluminal attenuation gradient (TAG) to define boundary conditions also showed good results, with the diagnostic accuracy of 91% with sensitivity of 89% and specificity of 91% [25]. Besides CFD-based approaches, Gao et. al. proposed a deep neural network solution (TreeVes-Net) that allows obtaining FFR values directly from static coronary CT angiography images, with AUC = 0.92 for detecting FFR  $\leq$  0.8 [26]. In addition, blood was generally modelled as Newtonian fluid in most validated approaches, which was reliable because there was no essential difference in results between Newtonian and non-Newtonian fluid assumptions in large arteries [27, 28]. On the other hand, there were studies showing differences between non-Newtonian and Newtonian fluid flows [29, 30], and Toshiba proposed a CT-FFR technique with non-Newtonian fluid model [31], however, the diagnostic performance was not very good (accuracy of 83.9% with AUC of 0.88).

Our study demonstrated credible results using AccuFFR<sub>ct</sub> for exploring ischemia-causing stenosis comparing with above-mentioned works. The overall diagnostic accuracy of AccuFFR<sub>ct</sub> was 89.7% on the per-vessel basis, which is higher than that of FFR<sub>CT</sub> and cFFR. The sensitivity, specificity, PPV, and NPV were 90.5, 89.5, 76.0 and 96.2%, respectively, while those for FFR<sub>CT</sub> were 84%, 86%, 61%, and 95%, respectively.  $\mu$ CT-FFR showed good diagnostic performance with 1% higher accuracy, While AccuFFR<sub>ct</sub>

resulted in slightly better sensitivity. It should be noted that higher sensitivity means less false negatives, which were critical in clinical application because false-negative results might put patients in danger for wasting the best treatment time. AccuFFRct showed an AUC of 0.945 for a per-patient basis and 0.925 per-vessel basis for categorizing functionally significant stenoses. The AUCs for FFR<sub>CT</sub>, cFFR, ML-based cFFR,  $\mu$ CT-FFR and TreeVes-Net-based FFR were 0.9, 0.92, 0.84, 0.92, 0.92, respectively. One cannot say AccuFFRct was superior in defining ischemia, but AccuFFRct did show very competitive results among similar works, and the diagnostic performance could be further optimized with future studies focusing on computational condition settings and algorithms, etc.

Except for the good diagnostic performance of AccuFFRct, the advantage of AccuFFRct lies in its time-efficient and convenient workflow. The application of FFR<sub>CT</sub> requires significant computational time (1–4 h) due to the need of data transfer to off-site supercomputers [11]. Workstation-based cFFR takes approximately 40 min with ML-based CT-FFR and 43 min with the reduced-order CFD-based CT-FFR [12, 15, 24, 32, 33]. As for AccuFFRct, only 35 min is required for the whole workflow, including 3D reconstruction of coronary artery geometry and CFD simulation, on average. Time efficiency is a critical factor for patients with coronary stenosis during the diagnostic procedure, because the time allowed for them varies from several minutes to weeks depending on their symptoms and the severity of ischemia, so it is important to shorten the diagnostic time for helping more patients during a fixed time. Moreover, a new ML-based algorithm for 3D reconstruction is under development, the total duration of AccuFFRct calculation will be reduced to about 10 min in the coming new version.

Though invasive FFR measurement is relatively safe in clinical use, risks and other limitations are still inevitable. Kumsars et al. [34] reported that about 1/10 of FFR could not be obtained due to side branches or wiring failure. Moreover, the high price of pressure wires may become a financial burden for patients. As a result, advanced computational analytical approaches that can compute FFR values from CCTA images alone could lead to widespread clinical utilization. AccuFFRct offers a time-efficient and accurate tool for FFR computation, and the visualized anatomic geometry of coronary tree can be used for subsequent clinical planning.

The main limitation of this study is its relatively small sample size with all CCTA data from a single center. A multi-centered study with large sample size is necessary to validate AccuFFRct further. In this study, the workflow and analysis were all performed by professionals. Thus training of normal medical staff is essential to ensure reliable execution of AccuFFRct analysis.

## Conclusions

The novel CFD-based CT-FFR method, AccuFFRct, is influential in determining significant functional CAD in a time-efficient manner with good diagnostic performance. It may emerge as a safe, efficient, and credible tool for evaluating coronary stenosis severity during diagnostic CCTA. In the future, algorithms would be continuously updated, some computational conditions or assumptions could also be optimized to assure clinically reliable results and to help more patients. A multicenter prospective clinical trial would be conducted to study the accuracy and clinical suitability of the algorithm for different types of stenosis, such as left main lesion, tandem lesion and bifurcation lesion.

## Methods

### Study design

This was a retrospective, observational, analytical study conducted at The Second Affiliated Hospital of Zhejiang University School of Medicine. Patients who had undergone coronary computed tomography angiography (CCTA) and invasive FFR measurements within 2 months were included. This study was approved by the Institutional Review Board of the hospital and informed consent of the patients was waived.

### Study population

The study population comprised 54 stable patients with suspected or known CAD who underwent CCTA and FFR measurements between January 2016 and September 2017. Exclusion criteria included individuals with prior myocardial infarction, prior coronary artery bypass surgery (CABG), prior stenting at the lesion of interest, significant motion or blurring artifact in CCTA, occlusion in any major coronary artery.

### CCTA acquisition and analysis

CCTA was performed using a dual-source 128-slice CT scanner (Somatom Definition FLASH, Siemens, Forchheim, Germany). Medications were administered individually and different CCTA scan modes were chosen according to patients' heart rate conditions. The tube voltage and tube current were set based on the body mass index of the patients. All CT images were reconstructed with a slice thickness of 0.5 mm. The CCTA image data was assessed in the central AccuFFRct core laboratory (ArteryFlow Technology Co., Ltd., Hangzhou, China) and selected for subsequent AccuFFRct calculation and analysis. The flowchart of this study is displayed in Fig. 5.

### ICA and FFR measurement

Invasive coronary angiography (ICA) was performed within 30 days after the CCTA acquisition according to standard practice. FFR measurements were conducted after inducing the maximum hyperemia by intravenous injection of adenosine at 180  $\mu\text{g}/\text{kg}/$

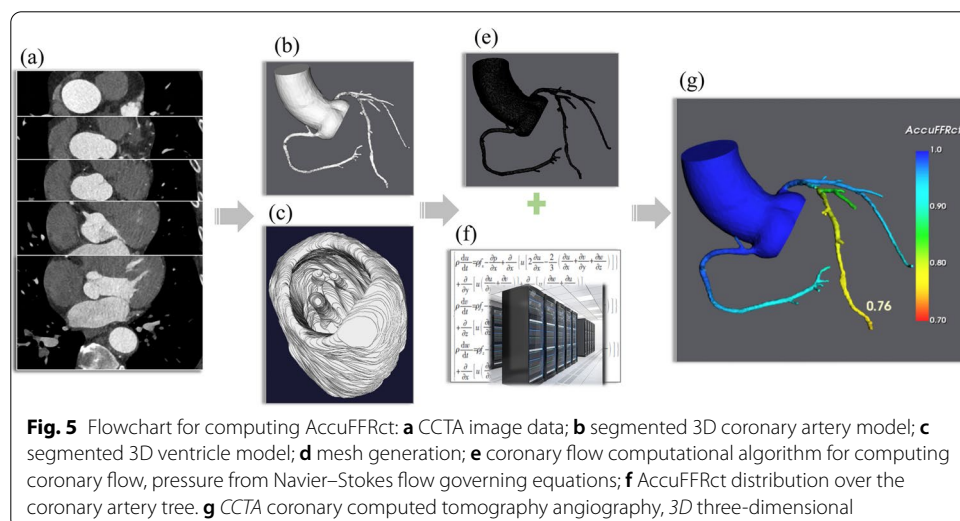


**Fig. 5** Flowchart for computing AccuFFRct: **a** CCTA image data; **b** segmented 3D coronary artery model; **c** segmented 3D ventricle model; **d** mesh generation; **e** coronary flow computational algorithm for computing coronary flow, pressure from Navier–Stokes flow governing equations; **f** AccuFFRct distribution over the coronary artery tree. **g** CCTA coronary computed tomography angiography, 3D three-dimensional



min. FFR was defined by dividing the mean pressure distal to the lesion by the mean aortic pressure under hyperemic condition, and an FFR value of  $\leq 0.80$  was considered hemodynamically significant. FFR data were transferred to the central AccuFFRct core laboratory for the following analysis by independent, blinded readers.

### CFD-based AccuFFRct computation

Using the most recent AccuFFRct analysis software (AccuFFR<sup>®</sup>ct, version 1.0, Artery-Flow), analysis was performed in a blinded fashion in the central AccuFFRct core laboratory.

The calculation of AccuFFRct includes four steps:

#### 1. Anatomical model reconstruction and segmentation

In this step, the anatomical geometry model of coronary arteries and ventricles can be obtained accurately from CCTA image data. First of all, the fast marching algorithm and colliding fronts algorithm were applied to segment aorta and coronary tree, differentiating them from other anatomic parts which were also include in CCTA image data. Subsequently, the optimal vessel borders were identified using the level-set method base on segmented CCTA images to ensure the real vessel shape. Then with an automatic geometry cleaning algorithm, the anatomical model of the coronary tree was obtained by marching cubes method [35] and the left ventricle model was extracted by a deep-learning segmentation method based on an 8-layer residual U-Net to compute the myocardium volume further. As shown in Fig. 5a–c.

In addition, though the CT images included in this study were relatively good, general CT data that meet the standard of Digital Imaging and Communications in Medicine (DICOM) with a slice thickness  $< 1$  mm is compatible with AccuFFRct, which means our technique can be used in numerous hospitals.

#### 2. Mesh generation and boundary conditions

The anatomical model of coronary arteries should be pre-processed, including hole checking, smoothing, boundary face editing of the 3D model, and then it would be transformed into a mesh model for later numerical CFD simulation to obtain the flow field of blood. In general, millions of mesh elements with different sizes were generated based on the structure of an anatomical model. In general, the maximum mesh size was limited as 0.3 mm for the best balance of computational precision and time based on previous mesh sensitivity tests, coarser mesh may lead to bigger error. Boundary conditions were the physical and physiological conditions applied to the mesh model to simulate the interaction between coronary arteries and related body parts. In this study, the patient-specific blood flow and aortic pressure were set as the inlet boundary condition. The resting blood flow was estimated by myocardium mass ( $Q \propto M^k$ ) and the flow rate was 2–4 times of resting condition at hyperemia. The blood flow rate at the outlet of each branch was calculated using Murray's law ( $Q_i \propto d^3$ ), and the rigid wall with no-slip boundary condition was applied to the vessel wall.

### 3. CFD simulation

The flow field information, including pressure and velocity at each mesh element, could be calculated by solving the fluid governing Navier–Stokes equations using the finite volume method. In this study, blood was modeled as Newtonian fluid (density  $\rho = 1056 \text{ kg/m}^3$ , viscosity  $\mu = 0.0035 \text{ Pa}\cdot\text{s}$ ) and incompressible [27], a modified solver based on an open-source CFD package (OpenFOAM 7) was used for this simulation of coronary blood flow.

### 4. AccuFFRct computation

The AccuFFRct value was calculated as the ratio of the distal pressure located at the measuring point of FFR to the mean aortic pressure. The simulation time for each case was approximately 35 min on a standard desktop, including the time of 3D reconstruction and CFD computation using AccuFFRct software.

### Statistical analysis

Continuous variables were presented as means  $\pm$  standard deviations or median in case of non-normal distribution. Categorical variables were presented as frequencies and percentages. The diagnostic performance of AccuFFRct (the ability of AccuFFRct to predict whether the  $\text{FFR} \leq 0.80$  or  $\text{FFR} > 0.80$ , i.e., whether the lesion would cause ischemia or not) was evaluated by calculating sensitivity, specificity, PPV, NPV and overall accuracy. Using FFR as a reference standard, sensitivity was defined by true positives divided by the sum of all true-positive and false-negative cases, specificity was defined as true negatives divided the sum of all true-negative and false-positive cases,  $\text{PPV} = \text{TP}/(\text{TP} + \text{FP})$ ,  $\text{NPV} = \text{TN}/(\text{TN} + \text{FN})$  and  $\text{accuracy} = (\text{TP} + \text{TN})/(\text{TP} + \text{FP} + \text{TN} + \text{FN})$ . Pearson correlation was used to quantify the degree of correlation between invasive FFR and AccuFFRct in detecting ischemia-causing stenoses. The area under the curve (AUC) derived from receiver-operating characteristic (ROC) curve analysis were computed using invasive FFR as the reference standard for checking classification performance (positive or negative for ischemia-causing) of AccuFFRct. The Bland–Altman statistics were also performed to assess the agreement of FFR and AccuFFRct. A two-sided P value of less than 0.05 was considered statistically significant. All statistical analyses were performed using MedCalc (MedCalc Software Inc., Belgium).

### Abbreviations

PCI: Percutaneous coronary intervention; CABG: Coronary artery bypass grafting; CCTA: Coronary computed tomography angiography; CAD: Coronary artery disease; 3D: Three-dimensional; CT: Computed tomography; CFD: Computational fluid dynamics; ICA: Invasive coronary angiography; FFR: Fractional flow reserve; ML: Machine learning; PPV: Positive predictive value; NPV: Negative predictive value; AUC: Area under the curve; ROC: Receiver operating characteristic.

### Authors' contributions

Conception and design or analysis and interpretation of data, or both: all authors. Drafting of the manuscript: YMH. Revising it critically for important intellectual content: WBJ, YBP, CLL, JPX. Final approval of the manuscript submitted: all authors.

### Funding

This work was supported by the National Natural Science Foundation of China (NO. 81320108003, NO. 31371498, NO. 81100141 and 81570322), Zhejiang Provincial Public Welfare Technology Research Project (NO. LGF20H020012), Zhejiang Provincial key research and development plan (NO. 2020C03016), the Major projects in Wenzhou of China (NO. ZY2019006), the Major projects in Jinhua of China (NO. 2020A31003) and Scientific research project of Zhejiang Education Department (NO. Y201330290).

**Availability of data and materials**

The datasets used and analyzed during the current study are available from the corresponding author on reasonable request.

**Declarations****Ethical approval and consent to participate**

Approval from an ethical review board of the hospitals was obtained before commencing the study.

**Consent for publication**

Not applicable.

**Conflicts of interest**

The authors confirm that no conflict of interest or any financial relationship related to the manuscript's content has been associated with this publication.

**Author details**

<sup>1</sup>Department of Cardiology, The Third Clinical Institute Affiliated to Wenzhou Medical University, Wenzhou, China. <sup>2</sup>ArteryFlow Technology Co., Ltd, Hangzhou, China. <sup>3</sup>Department of Cardiology, The Second Affiliated Hospital of Zhejiang University School of Medicine, 88 Jiefang Road, Hangzhou 310009, China. <sup>4</sup>Department of Cardiology, Affiliated Jinhua Hospital, Zhejiang University School of Medicine, Jinhua, China.

Received: 5 May 2021 Accepted: 26 July 2021

Published online: 04 August 2021

**References**

1. Min JK, Shaw LJ, Berman DS. The present state of coronary computed tomography angiography. *J Am Coll Cardiol.* 2010;55(10):957–65.
2. Meijboom WB, Van Mieghem CAG, van Pelt N, Weustink A, Pugliese F, Mollet NR, et al. Comprehensive assessment of coronary artery stenoses: computed tomography coronary angiography versus conventional coronary angiography and correlation with fractional flow reserve in patients with stable angina. *J Am Coll Cardiol.* 2008;52(8):636–43.
3. Tonino PAL, De Bruyne B, Pijls NHJ, Siebert U, Ikeno F, van 't Veer M, et al. Fractional flow reserve versus angiography for guiding percutaneous coronary intervention. *N Engl J Med.* 2009;360(3):213–24. <https://doi.org/10.1056/NEJMo a0807611>.
4. Kern MJ, Samady H. Current concepts of integrated coronary physiology in the catheterization laboratory. *J Am Coll Cardiol.* 2010. <https://doi.org/10.1016/j.jacc.2009.06.062>.
5. Pijls NHJ, de Bruyne B, Peels K, van der Voort PH, Bonnier HJRM, Bartunek J, et al. Measurement of fractional flow reserve to assess the functional severity of coronary-artery stenoses. *N Engl J Med.* 1996;334(26):1703–8.
6. Members TF, Montalescot G, Sechtem U, Achenbach S, Andreotti F, Arden C, et al. 2013 ESC guidelines on the management of stable coronary artery disease: The Task Force on the management of stable coronary artery disease of the European Society of Cardiology. *Eur Heart J.* 2013;34(38):2949–3003. <https://doi.org/10.1093/eurheartj/ehv296>.
7. De Bruyne B, Pijls NHJ, Kalesan B, Barbato E, Tonino PAL, Piroth Z, et al. Fractional flow reserve-guided PCI versus medical therapy in stable coronary disease. *N Engl J Med.* 2012;367(11):991–1001. <https://doi.org/10.1056/NEJMo a1205361>.
8. Taylor CA, Fonte TA, Min JK. Computational fluid dynamics applied to cardiac computed tomography for noninvasive quantification of fractional flow reserve. *J Am Coll Cardiol.* 2013;61(22):2233–41.
9. Koo B-K, Erglis A, Doh J-H, Daniels DV, Jegere S, Kim H-S, et al. Diagnosis of ischemia-causing coronary stenoses by noninvasive fractional flow reserve computed from coronary computed tomographic angiograms. *J Am Coll Cardiol.* 2011;58(19):1989–97.
10. Min JK, Leipsic J, Pencina MJ, Berman DS, Koo B-K, van Mieghem C, et al. Diagnostic accuracy of fractional flow reserve from anatomic CT angiography. *JAMA.* 2012;308(12):1237. <https://doi.org/10.1001/2012.jama.11274>.
11. Nørgaard BL, Leipsic J, Gaur S, Seneviratne S, Ko BS, Ito H, et al. Diagnostic performance of noninvasive fractional flow reserve derived from coronary computed tomography angiography in suspected coronary artery disease. *J Am Coll Cardiol.* 2014;63(12):1145–55.
12. Tesche C, De Cecco CN, Albrecht MH, Duguay TM, Bayer RR, Litwin SE, et al. Coronary CT Angiography–derived fractional flow reserve. *Radiology.* 2017;285(1):17–33. <https://doi.org/10.1148/radiol.2017162641>.
13. Goldstein JA, Gallagher MJ, O'Neill WW, Ross MA, O'Neil BJ, Raff GL. A randomized controlled trial of multi-slice coronary computed tomography for evaluation of acute chest pain. *J Am Coll Cardiol.* 2007. <https://doi.org/10.1016/j.jacc.2006.08.064>.
14. Ko BS, Cameron JD, Munnur RK, Wong DTL, Fujisawa Y, Sakaguchi T, et al. Noninvasive CT-Derived FFR based on structural and fluid analysis. *JACC Cardiovasc Imaging.* 2017;10(6):663–73.
15. Coenen A, Lubbers MM, Kurata A, Kono A, Dedic A, Chelu RG, et al. Fractional flow reserve computed from noninvasive CT angiography data: diagnostic performance of an on-site clinician-operated computational fluid dynamics algorithm. *Radiology.* 2014;274(3):674–83. <https://doi.org/10.1148/radiol.14140992>.
16. Douglas PS, Pontone G, Hlatky MA, Patel MR, Nørgaard BL, Byrne RA, et al. Clinical outcomes of fractional flow reserve by computed tomographic angiography-guided diagnostic strategies vs usual care in patients with suspected coronary artery disease: the prospective longitudinal trial of FFRCT: outcome and resource impacts stud. *Eur Heart J.* 2015;36(47):3359–67. <https://doi.org/10.1093/eurheartj/ehv444>.

17. Driessen RS, Danad I, Stuijzand WJ, Rajmakers PG, Schumacher SP, van Diemen PA, et al. Comparison of coronary computed tomography angiography, fractional flow reserve, and perfusion imaging for ischemia diagnosis. *J Am Coll Cardiol*. 2019. <https://doi.org/10.1016/j.jacc.2018.10.056>.
18. Hlatky MA, Saxena A, Koo B-K, Erglis A, Zarins CK, Min JK. Projected costs and consequences of computed tomography-determined fractional flow reserve. *Clin Cardiol*. 2013;36(12):743–8. <https://doi.org/10.1002/clc.22205>.
19. Fairbairn TA, Nieman K, Akasaka T, Nørgaard BL, Berman DS, Raff G, et al. Real-world clinical utility and impact on clinical decision-making of coronary computed tomography angiography-derived fractional flow reserve: lessons from the ADVANCE Registry. *Eur Heart J*. 2018;39(41):3701–11. <https://doi.org/10.1093/eurheartj/ehy530>.
20. Patel MR, Nørgaard BL, Fairbairn TA, Nieman K, Akasaka T, Berman DS, et al. 1-year impact on medical practice and clinical outcomes of FFRCT. *JACC Cardiovasc Imaging*. 2020. <https://doi.org/10.1016/j.jcmg.2019.03.003>.
21. Renker M, Schoepf UJ, Wang R, Meinel FG, Rier JD, Bayer RR, et al. Comparison of diagnostic value of a novel noninvasive coronary computed tomography method versus standard coronary angiography for assessing fractional flow reserve. *Am J Cardiol*. 2014;114(9):1303–8.
22. Baumann S, Wang R, Schoepf UJ, Steinberg DH, Spearman JV, Bayer RR, et al. Coronary CT angiography-derived fractional flow reserve correlated with invasive fractional flow reserve measurements—initial experience with a novel physician-driven algorithm. *Eur Radiol*. 2015;25(4):1201–7. <https://doi.org/10.1007/s00330-014-3482-5>.
23. Itu L, Rapaka S, Passerini T, Georgescu B, Schwemmer C, Schoebinger M, et al. A machine-learning approach for computation of fractional flow reserve from coronary computed tomography. *J Appl Physiol*. 2016;121(1):42–52. <https://doi.org/10.1152/jappphysiol.00752.2015>.
24. Adriaan C, Young-Hak K, Mariusz K, Christian T, Jakob DG, Akira K, et al. Diagnostic accuracy of a machine-learning approach to coronary computed tomographic angiography-based fractional flow reserve. *Circ Cardiovasc Imaging*. 2018;11(6):e007217. <https://doi.org/10.1161/CIRCIMAGING.117.007217>.
25. Tang CX, Liu CY, Lu MJ, Schoepf UJ, Tesche C, Bayer RR, et al. CT FFR for ischemia-specific CAD with a new computational fluid dynamics algorithm. *JACC Cardiovasc Imaging*. 2020;13(4):980–90.
26. Gao Z, Wang X, Sun S, Wu D, Bai J, Yin Y, et al. Learning physical properties in complex visual scenes: an intelligent machine for perceiving blood flow dynamics from static CT angiography imaging. *Neural Netw*. 2020;123:82–93.
27. Perktold K, Peter R, Resch M. Pulsatile non-Newtonian blood flow simulation through a bifurcation with an aneurysm. *Biorheology*. 1989;26(6):1011–30. <https://doi.org/10.3233/BIR-1989-26605>.
28. Johnston BM, Johnston PR, Corney S, Kilpatrick D. Non-newtonian blood flow in human right coronary arteries: transient simulations. *J Biomech*. 2006;39(6):1116–28. <https://doi.org/10.1007/s12573-011-0040-5>.
29. Chen J, Lu X-Y, Wang W. Non-Newtonian effects of blood flow on hemodynamics in distal vascular graft anastomoses. *J Biomech*. 2006;39(11):1983–95.
30. Apostolidis AJ, Moyer AP, Beris AN. Non-Newtonian effects in simulations of coronary arterial blood flow. *J Nonnewton Fluid Mech*. 2016;233:155–65. <https://doi.org/10.1016/j.jnnfm.2016.03.008>.
31. Ko BS, Cameron JD, Munnur RK, Wong DTL, Fujisawa Y, Sakaguchi T, et al. Noninvasive CT-Derived FFR based on structural and fluid analysis: a comparison with invasive ffr for detection of functionally significant stenosis. *JACC Cardiovasc Imaging*. 2017;10(6):663–73.
32. Coenen A, Lubbers MM, Kurata A, Kono A, Dedic A, Chelu RG, et al. Coronary CT angiography derived fractional flow reserve: methodology and evaluation of a point of care algorithm. *J Cardiovasc Comput Tomogr*. 2016;10(2):105–13.
33. Tesche C, De Cecco CN, Baumann S, Renker M, McLaurin TW, Duguay TM, et al. Coronary CT angiography-derived fractional flow reserve: machine learning algorithm versus computational fluid dynamics modeling. *Radiology*. 2018;288(1):64–72. <https://doi.org/10.1148/radiol.2018171291>.
34. Kumsars I, Narbutė I, Thuessen L, Niemelä M, Steigen TK, Kervinen K, et al. Side branch fractional flow reserve measurements after main vessel stenting: a Nordic-Baltic Bifurcation Study III substudy. *EuroIntervention*. 2012;7(10):1155–61. <https://doi.org/10.4244/EIJV7I10A186>.
35. Xiang J, Antiga L, Varble N, Snyder KV, Levy EI, Siddiqui AH, et al. AVIEW: an image-based clinical computational tool for intracranial aneurysm flow visualization and clinical management. *Ann Biomed Eng*. 2016;44(4):1085–96. <https://doi.org/10.1007/s10439-015-1363-y>.

## Publisher's Note

Springer Nature remains neutral with regard to jurisdictional claims in published maps and institutional affiliations.

Ready to submit your research? Choose BMC and benefit from:

- fast, convenient online submission
- thorough peer review by experienced researchers in your field
- rapid publication on acceptance
- support for research data, including large and complex data types
- gold Open Access which fosters wider collaboration and increased citations
- maximum visibility for your research: over 100M website views per year

At BMC, research is always in progress.

Learn more [biomedcentral.com/submissions](https://biomedcentral.com/submissions)

